25th ABCM International Congress of Mechanical Engineering
October 20-25, 2019, Uberlândia, MG, Brazil

Effects of 3D printing variability on the vibration attenuation of metamaterial beams

Adriano T. Fabro
Department of Mechanical Engineering, University of Brasilia, Brasilia, DF, 70910-900, Brazil
fabro@unb.br

Danilo Beli
Department of Aeronautical Engineering, Sao Carlos School of Engineering, Sao Carlos, SP, 13563-120, Brazil

Massimo Ruzzenne
Daniel Guggenhein School of Aerospace Engineering and George W. Woodruff School of Mechanical Engineering, Georgia Institute of Technology, Atlanta, GA, 30332, USA

Jose Roberto F. Arruda
School of Mechanical Engineering, University of Campinas, Cidade Universitaria, Campinas, SP, 13083-860, Brazil

Abstract. *In this work, the physical effects of the material variability on the attenuation performance of metamaterial beams is investigated experimentally and numerically. The additive manufacturing produces spatially correlated uncertainty for the material properties, which breaks the translational periodicity affecting the wave propagation performance of the periodic structures. The wave attenuation is analysed in the beams individually and in ensemble, and it is shown that the attenuation bandwidth increases until an optimal disorder. After that, the band gap mistuning loses vibration attenuation performance. In addition, it is also shown that the variability induces wave trapping, which is created by the band gap tailoring in space and depends on the excitation location. These two interesting physical phenomena, bandwidth widening and wave trapping, were experimentally observed in metastructures constructed from 3D printing. This study illustrates the physical consequences of the variability on the wave propagation of metamaterials constructed in additive manufacturing when compared to the periodic nominal design.*

Keywords: *metamaterial, uncertainty, wave trapping, additive manufacturing*

1. INTRODUCTION

Metamaterials are periodic structures that have been used to control and to manipulate acoustic and elastic waves through band gaps, i.e. frequency bands with no wave propagation (Brillouin, 1953; Lu *et al.*, 2009; Maldovan, 2013; Hussein *et al.*, 2014; Ma and Sheng, 2016). In metamaterials, the band gap effect is created by Mie-type or Fabry-Perot-type resonances due to inclusions functioning as local resonators (Liu *et al.*, 2000; Zhu *et al.*, 2010). In addition, 3D printing has become one of the emerging topics in metamaterials because it allows for intrinsically complex geometry to produce local resonators (Bertoldi *et al.*, 2017). However, manufacturing processes introduce material and geometric variabilities (Hague *et al.*, 2003; Goodridge *et al.*, 2012), which break the translational periodicity, mistuning the band gaps of each the unit cells, and affecting the wave propagation performance in the periodic structure.

Wave-based methods have been used to calculate the complex dispersion diagram (free wave analysis) and the forced response in the frequency domain of a finite length periodic structures. These approach is computationally more efficient when compared to the standard full Finite Element (FE) method thus providing a suitable framework for optimization and uncertainty analysis (Meng *et al.*, 2019). In the past decades, the Spectral Element (SE) Doyle (1997); Lee (2009) approach and Wave and Finite Element (WFE) method Mace *et al.* (2005); Mencik and Ichchou (2005); Renno and Mace (2010) have been successfully used to model homogeneous and periodic structures. More recently, a numerical approach based on the WFE and SE was proposed for slowly varying waveguides and near-periodic structures (Fabro *et al.*, 2019, 2016a). Near-periodic structures are referred herein as systems where material or geometric properties vary spatially following a deterministic function or a random field (Vanmarcke, 2010). This disruption of the spatial periodicity is known as disorder and results in the phenomenon known as localization Anderson (1958).

In this work, further discussion is provided on the results by Beli *et al.* (2019), in which a set of metamaterial beams were produced from additive manufacturing. For each beam, the local material properties could be estimated and a link between the dynamic response and material distributions could be established such that a deeper understanding on the

physical phenomenons produced by the variability can be set. To further understand the results, numerical experiments are proposed in terms of phase and attenuation change assuming slowly varying changes on the resonators. It is shown that the attenuation bandwidth can be enlarged or annihilated, in which the resonators profile play a major role and can also lead to wave trapping phenomena.

2. DETERMINISTIC ANALYSIS BY A WAVE-BASED APPROACH

This section reviews a formulation for wave propagation in periodic structures in terms of the dynamic stiffness of a single unity cell. Moreover, it presents a formulation introduced by Fabro et al. (Fabro *et al.*, 2016b, 2019) for the forced response of non-homogeneous waveguides with slowly varying properties, which is then applied for nearly-periodic structures.

2.1 COMPLEX FREE WAVE PROPAGATION ALONG A PERIOD STRUCTURE: $k(\omega)$ EIGENVALUE PROBLEM

The first step is modelling the unit cell with SE (Doyle, 1997; Lee *et al.*, 2007). An unit cell with one-dimensional periodicity is considered where left (L), right (R) and interior (I) degrees of freedom (DOFs) are presented. The equations of motion for the s^{th} unit cell described on frequency domain is $\widetilde{\mathbf{D}}\hat{\mathbf{q}} = \hat{\mathbf{f}}$, where $\hat{\mathbf{q}}$ is the discrete displacement/rotation vector composed by all degrees of freedom, $\hat{\mathbf{f}}$ is the vector of correspondent internal efforts and $\hat{(\ )}$ represents the time harmonic description. If no external forces are applied on interior DOFs, $\hat{\mathbf{f}}_{\mathtt{I}} = \mathbf{0}$, these DOFs can be related to the left and right interface DOFs by $\hat{\mathbf{q}}_{\mathtt{I}} = -\widetilde{\mathbf{D}}_{\mathtt{II}}^{-1}(\widetilde{\mathbf{D}}_{\mathtt{IL}}\hat{\mathbf{q}}_{\mathtt{L}} + \widetilde{\mathbf{D}}_{\mathtt{IR}}\hat{\mathbf{q}}_{\mathtt{R}})$ (Duhamel *et al.*, 2006) and a condensed dynamic stiffness matrix is obtained

$$\begin{bmatrix} \mathbf{D}_{\mathtt{LL}} & \mathbf{D}_{\mathtt{LR}} \\ \mathbf{D}_{\mathtt{RL}} & \mathbf{D}_{\mathtt{RR}} \end{bmatrix} \begin{bmatrix} \hat{\mathbf{q}}_{\mathtt{L}} \\ \hat{\mathbf{q}}_{\mathtt{R}} \end{bmatrix} = \begin{bmatrix} \hat{\mathbf{f}}_{\mathtt{L}} \\ \hat{\mathbf{f}}_{\mathtt{R}} \end{bmatrix}, \tag{1}$$

where $\mathbf{D}_{\mathtt{BB}} = \widetilde{\mathbf{D}}_{\mathtt{BB}} - \widetilde{\mathbf{D}}_{\mathtt{BI}}\widetilde{\mathbf{D}}_{\mathtt{II}}^{-1}\widetilde{\mathbf{D}}_{\mathtt{IB}}$, with $\mathtt{B} = [\mathtt{L} \quad \mathtt{R}]$.

By assuming the periodic structure free of external forces, the compatibility of displacements as well as the equilibrium of internal forces at interface of two consecutive unit cells are given by $\hat{\mathbf{q}}_{\mathtt{R}}^{(s)} = \hat{\mathbf{q}}_{\mathtt{L}}^{(s+1)}$ and $\hat{\mathbf{f}}_{\mathtt{R}}^{(s)} = -\hat{\mathbf{f}}_{\mathtt{L}}^{(s+1)}$, respectively. In addition, the state vector of two consecutive identical interfaces can be related by a transfer matrix which is written in terms of the condensed dynamic stiffness matrix as $\mathbf{u}^{(s+1)} = \mathbf{T}\mathbf{u}^{(s)}$, where

$$\mathbf{T} = \begin{bmatrix} -\mathbf{D}_{\mathtt{LR}}^{-1}\mathbf{D}_{\mathtt{LL}} & \mathbf{D}_{\mathtt{LR}}^{-1} \\ -\mathbf{D}_{\mathtt{RL}} + \mathbf{D}_{\mathtt{RR}}\mathbf{D}_{\mathtt{LR}}^{-1}\mathbf{D}_{\mathtt{LL}} & -\mathbf{D}_{\mathtt{RR}}\mathbf{D}_{\mathtt{LR}}^{-1} \end{bmatrix}, \quad \mathbf{u}^{(s+1)} = \begin{bmatrix} \hat{\mathbf{q}}_{\mathtt{L}}^{(s+1)} \\ \hat{\mathbf{f}}_{\mathtt{L}}^{(s+1)} \end{bmatrix} \quad \text{and} \quad \mathbf{u}^{(s)} = \begin{bmatrix} \hat{\mathbf{q}}_{\mathtt{L}}^{(s)} \\ \hat{\mathbf{f}}_{\mathtt{L}}^{(s)} \end{bmatrix}.$$

If the dynamic stiffness matrix is symmetric then $\mathbf{T}$ is symplectic; moreover, $\mathbf{T}$ is $\Delta-$periodic (Δ is the length of unit cell), which makes this matrix invariant under a translation of length Δ (Mencik and Ichchou, 2008). Due to the periodicity, Bloch's theorem can be applied to relate the state vectors of two consecutive interfaces, $\mathbf{u}^{(s+1)} = \lambda\mathbf{u}^{(s)}$, where $\lambda_j = e^{-\mathrm{i}\mu_j}$, where μ_j is the propagation constant. Therefore, the eigenvalue problem in becomes$\mathbf{T}\boldsymbol{\phi}_j = \lambda_j\boldsymbol{\phi}_j$.

The previous eigenproblem provides $2n$ eigensolutions, where n corresponds to the number of DOF associated with each interface. While the eigenvalues (λ_j) are associated to phase change or attenuation along the structure length, the eigenvectors or wave mode shapes ($\boldsymbol{\phi}_j$) indicate the spatial distribution of the displacements and forces on the cross section Mace *et al.* (2005). The wave modes appear in pairs (λ_j^+, $\boldsymbol{\phi}_j^+$) and (λ_j^-, ϕ_j^-), which are related to the right-going and left-going waves, respectively. Also, because $\widetilde{\mathbf{D}}$ is symmetric, the eigenvalues related to forward and backward going waves are linked by $\lambda_j^- = 1/\lambda_j^+$. Moreover, the eigenvectors can be partitioned in displacement and force components as $\boldsymbol{\phi}_j^{\mathtt{T}} = [\boldsymbol{\phi}_{qj}^{\mathtt{T}} \quad \boldsymbol{\phi}_{fj}^{\mathtt{T}}]$ and the right-going waves are defined such that $|\lambda_j^+| \leq 1$ and $\Re\{i\omega\boldsymbol{\phi}_{fj}^{\mathtt{T}}\boldsymbol{\phi}_{qj}\} < 0$ if $|\lambda_j^+| = 1$.

2.2 NEARLY-PERIODIC STRUCTURES WITH SLOWLY VARYING PROPERTIES

In this section, the procedure to compute the phase and amplitude change of travelling waves on nearly-periodic structures with slowly varying properties is briefly presented, base on (Fabro *et al.*, 2016a). Assuming a time harmonic motion, a linear transformation can be used to relate the physical domain to the wave amplitude domain (Renno and Mace, 2010)

$$\hat{\mathbf{q}}_{\mathtt{L}} = \boldsymbol{\Phi}_{\mathtt{q}}^{+}\mathbf{a}^{+} + \boldsymbol{\Phi}_{\mathtt{q}}^{-}\mathbf{a}^{-} \quad \text{and} \quad \hat{\mathbf{f}}_{\mathtt{L}} = \boldsymbol{\Phi}_{\mathtt{f}}^{+}\mathbf{a}^{+} + \boldsymbol{\Phi}_{\mathtt{f}}^{-}\mathbf{a}^{-}, \tag{2}$$

in terms of the positive going $\mathbf{a}^+$ and negative going $\mathbf{a}^-$ wave amplitudes, and the matrices $\boldsymbol{\Phi}_{\mathtt{q}}^{\pm} = [\boldsymbol{\phi}_{q1}^{\pm} \cdots \boldsymbol{\phi}_{qm}^{\pm}]$ and $\boldsymbol{\Phi}_{\mathtt{f}}^{\pm} = [\boldsymbol{\phi}_{f1}^{\pm} \cdots \boldsymbol{\phi}_{fm}^{\pm}]$ are $n \times m$, where n is the number of DOF in the left interface and m corresponds to the number

of retained wavemodes. For a periodic structure, the wave modes are the same for any periodic cell while in the nearly periodic case they depend on the position. It is assumed that the positive and negative propagation matrices for waves travelling between 0 and L can be defined as Fabro *et al.* (2015)

$$\mathbf{\Lambda}^{+}(0,L) = \mathtt{diag}\left[\exp\left(-\mathrm{i}\theta_j(0,L) + \gamma_j(0,L)\right)\right] \tag{3}$$

$$\mathbf{\Lambda}^{-}(L,0) = \mathtt{diag}\left[\exp\left(-\mathrm{i}\theta_j(0,L) - \gamma_j(0,L)\right)\right], \tag{4}$$

where $\mathtt{diag}[\cdot]$ stands for diagonal matrix, $\theta_j(0,L)$ is the total phase change and wave attenuation of the j^{th} wave mode, given by

$$\theta_j(0,L) = \sum_{i=1}^{N} \Re\left[\mu_j(x_i)\right] + \mathrm{i}\sum_{i=1}^{N} \Im\left[\mu_j(x_i)\right], \tag{5}$$

with $\mu_j(x_i)$ being the locally defined propagation constant at the position x_i of the centre of the i^{th} unity cell. Moreover, $\Re\left[\mu_j(x_i)\right]$ is related to the phase change, $\Im\left[\mu_j(x_i)\right]$ is related to wave attenuation and damping and $\gamma_j(0,L)$ is the amplitude change caused by the non-periodic changes on the structure.

This assumption considers that negligible wave reflection occurs due to slowly varying near-periodicity. Moreover, it is also assumed that there are no critical sections, also known as turning points in the WKB approach, which can arise from the rapidly changing properties, due to waves cutting-on/off and due to waves veering or looking **?**. It can also be shown that this is equivalent to assuming that systems undergoes no localization (Luongo, 1992). Note that $\mathbf{\Lambda}^{+}(0,L) \neq \mathbf{\Lambda}^{-}(L,0)$, unlike the periodic case. The real part of $\theta_j(0,L)$ is related to the phase change and the imaginary part of $\theta_j(0,L)$ is related to the wave attenuation due to damping. The SE method can be used to estimate a local propagation and respective wave modes.

Due to the slowly varying assumption, the locally defined propagation constant can be approximated to a continuously varying function $\mu_j(x_i) \approx \mu_j(x)$. This approximation can be done from a polynomial interpolation. Therefore, a numerical scheme such as the Gauss-Legendre (GL) quadrature is used to approximate the phase change as

$$\theta_j(0,L) \approx \sum_{m=1}^{N_{gl}} G_i \Re\left[\mu_j(x_m)\right] + \mathrm{i}\sum_{m=1}^{N_{gl}} G_i \Im\left[\mu_j(x_m)\right], \tag{6}$$

where G_i are the weights and $\mu_j(x_m)$ is the j^{th} propagation constant given at the sampling point x_m, defined from the GL quadrature, and N_{gl} is the number of integration points. This strategy is propose to keep the number of evaluations of the propagation constant to a minimum and then avoid excessive computational cost.

The amplitude change due to non-periodic changes on the structure can be calculated from energy conservation for an undamped system as a consequence of the WKB approximation (Pierce, 1970). It can be shown that the two approaches are equivalent to the leading order of the WKB approximation (Nielsen and Peake, 2016; Morsbol *et al.*, 2016). Therefore, for a positive-going wave travelling from x_a, with amplitude $\mathbf{a}^{+}$, to x_b, with amplitude $\mathbf{b}^{+}$, assuming no damping, the time average power transmitted through the cross-sections, at the two positions must be equal, leading to (Fabro *et al.*, 2019)

$$\gamma_j(0,L) = \frac{1}{2}\log\left\{\frac{\Re\left[\mathrm{i}\omega\boldsymbol{\phi}_{f,i}^{+H}(0)\boldsymbol{\phi}_{q,i}^{+}(0)\right]}{\Re\left[\mathrm{i}\omega\boldsymbol{\phi}_{f,i}^{+H}(L)\boldsymbol{\phi}_{q,i}^{+}(L)\right]}\right\}. \tag{7}$$

Note that, although the wave modes propagate independently, the wave mode shapes $\boldsymbol{\phi}_i^{\pm}(x)$ vary slowly along the structure. It is also assumed that light damping can be included straightforwardly by calculating the complex wavenumber $k_j(x)$ at each segment using the SE approach and then Eq. (6) is applied to calculate the total phase change and attenuation. In the following sections, this approach is applied to both a metastructure with nearly-periodic properties. The effects of the break of periodicity are investigated assuming slowly varying properties.

3. EXPERIMENTAL RESULTS: WAVE TRAPPING

The experimental results presented in this section have been published by Beli *et al.* (2019). Experimental investigations were performed in ten metastructure samples with the same nominal design in all unit cells and from which two are considered here. The experimental set-up is described in detail in (Beli *et al.*, 2019). The forced response measurements

and different vibration attenuation behaviours were observed among the samples. In addition, the material properties along the metastructure were obtained following the ultrasound experimental set-up and a significant spatial variation among the unit cells was observed.

The effects of breaking the periodicity by correlated deterministic variability on the band gap performance is investigated by selecting two cases, namely `MM1` and `MM4`. The dynamic responses of the four samples are shown in Fig. 1(a-b), where the green lines represent the spatial distribution of the elastic modulus and the blue lines are the band gap limits for each unity cell.

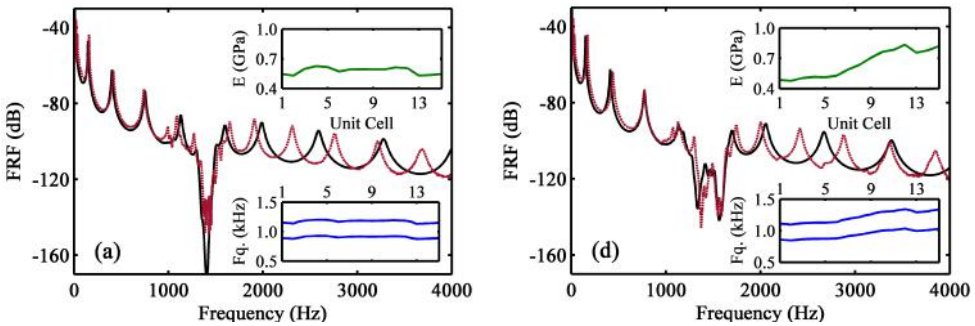

(a) (b)

Figure 1: Dynamic response for the metamaterial beam samples: `MM1` (a) and `MM4` (b). Legend: experimental measurement in 3D printing model (red), numerical simulation with FE model (black), experimental spatial distribution of elastic modulus (green) and band gap limits for each unit cell (blue). Adapted from (Beli *et al.*, 2019).

In the `MM1`, a small bandwidth ($\Delta f \approx 250$ Hz) with deep attenuation is observed, which is related to small spatial variation of the material properties. In the `MM4`, two attenuation regions ($\Delta f \approx 340$ Hz) are observed because the spatial distribution of elastic properties is very smooth from cells 1 to 5 and changes rapidly from cell 6 onwards and have two distinct levels, one with $E \approx 0.4$ GPa and another with $E \approx 0.7$ GPa. A slowly varying change on the material properties increases the attenuation bandwidth when compared to the rapidly change case. These experimental results show the high influence of the spatial distribution of material properties on the band gap performance.

The experimental FRFs are also compared to standard FE numerical simulations, using the material properties estimated experimentally. It can be noticed that for low frequencies and for the band gap zone, the numerical and experimental results are in a good agreement and the FE model captures the physical behaviour involved in the disorder. The FE validation confirms that the spatial distribution of material properties is responsible for the vibration attenuation performance of the dynamic response. The mismatch in the higher frequencies can be attributed to the simplicity of the beam model or to ortrotopy/anisotropy of the material properties. It requires further investigations beyond the scope of this paper. The resonator variability promotes a mistuning around the fundamental frequency which can lead, such as in phononic crystals with gradient index, to Anderson/energy localization (Luongo, 1992; del Barco and Ortuño, 2012) and wave trapping (Trainiti *et al.*, 2018; Hu *et al.*, 2013).

By imposing an excitation force at unit cell `0`, the measurement displacement as a function of space and frequency is shown in Fig. 2(a-b) for the two metastructures samples `MM1` and `MM4`. A well defined attenuation in space is achieved for `MM1`, the vibration localization close to the excitation occurs due the presence of a near field created by the point excitation. However, for `MM4`, the resonances around the band gap are mitigated through the space which produces a wave trapping. This effect appears because at a fixed frequency some of the resonators closer to the excitation are not absorbing energy from the host structure and some of resonators, far from excitation, are absorbing energy from the host structure. This effect can be explained from the change on the band gap limits as a function of the space, shown in Fig. 2(d). Moreover, a reflection interface is created at the transition between these two regions, creating a critical section, due to the local change from a propagating to a non-propagating wave. This is also know as a turning point (Biggs, 2012). Fig. 2(c,f) present the displacement along the metastructure for `MM1` and `MM4` samples for the frequency. Excitation at each end of the metastructure produces different vibration profiles. Excitation at cell `15` produced whole body vibration while excitation at cell `0` produces wave trapping between unit cells `10` and `15` and concentrates the vibration energy between unit cells `0` and `10`. Experimental results were validated with standard FE simulations.

4. NEARLY-PERIODIC METAMATERIAL

In this section, the variability on the resonators is numerically investigated from the phase and attenuation point of view. It has been for this kind of structure that variability on the properties of the host beam do not affect the band gap performance and it is unlikely to generate wave trapping (Fabro *et al.*, 2016a). The bending stiffness properties of the I-

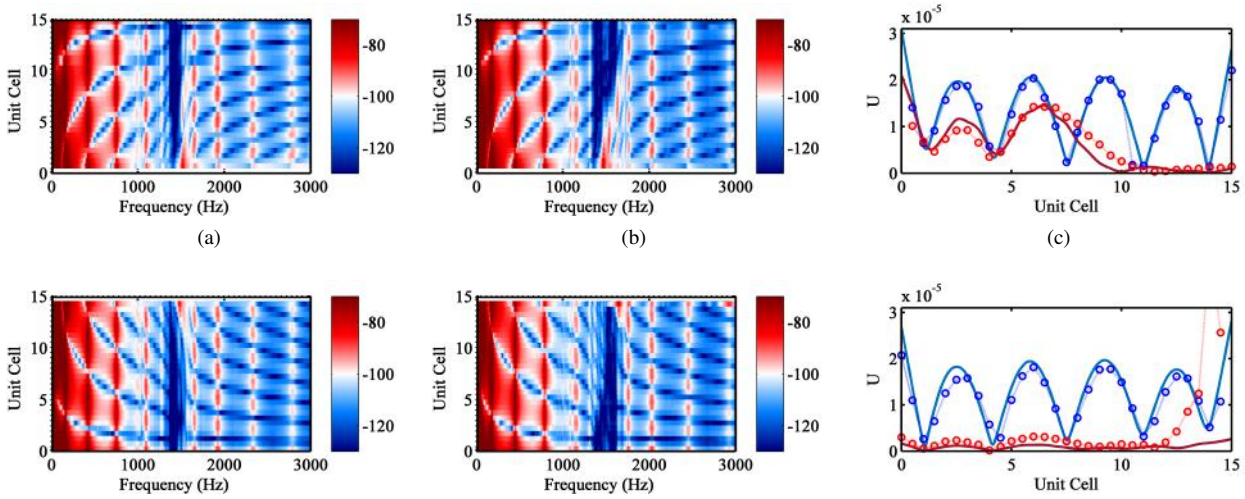

Figure 2: Experimental displacement amplitude as a function of space and frequency for the samples: `MM1` (a, d) and `MM4` (b, e), where the colors represent the displacement amplitude. Experimental (○) and FE numerical (–) observation of wave trapping by comparing the spatial displacement (c, f): `MM1` at $f = 1654$ Hz (blue) and `MM4` at $f = 1632$ Hz (red). Excitation location at unit cell `0` (a-c) and at unit cell `15` (d-f). Extracted from (Beli *et al.*, 2019).

beam and the resonators in the metamaterial beam are considered to be varying along the beam length. Recall that they are different from the I-beam to which they are attached. The case of a deterministic variability is investigated and the effects of the break of periodicity of the resonators in the band gap performance are analysed. For that end, a continuous function is used to represent the spatial variability, and then the property of the cell s is given by the value of the function at the centre of the cell x_S, i.e., the Young's modulus $E^{(s)} = E(x_s)$. This approximation holds for slowly varying properties.

The model studied herein consists of an I-beam with periodically attached resonators. The nominal geometric dimensions of the unit cell shown in Fig. 3 are $l_a = \Delta = 16$ mm, $l_b = 12$ mm, $l_c = 13$ mm, $l_d = 2$ mm, $l_e = 3$ mm, $l_f = 5$ mm, $l_g = 1$ mm and $l_h = 12$ mm. The global structure has 21 cells and is made of polyamide, whose nominal properties are shown in Table 1. These properties are slightly different from the metastructures in the previous section but their physical behaviour should be no different. Free boundary conditions are assumed at both ends. The resonators are attached to both sides of the web, and the additional mass due to the resonators is around 30% of the total mass of the beam.

A Timoshenko frame Spectral Element (Lee, 2009; Doyle, 1997) is used to model the resonator mass, a second one is used to model the resonator spring, Fig. 3(a). These elements have two nodes and six degrees of freedom (DOF) per node, three displacements and three rotations, which describe vertical bending, lateral bending, extension/compression and torsion dynamic effects. Two elements are used to model the I-beam, with the middle node connecting the resonator from both sides, as shown in Fig. 3(b). After the global matrix assembly and condensation of the interior nodes, a dynamic stiffness matrix is obtained, Eq. (1), and an eigenvalue problem can be set up as presented in Section 2. In the example treated here, there is no need to improve the numerical conditioning.

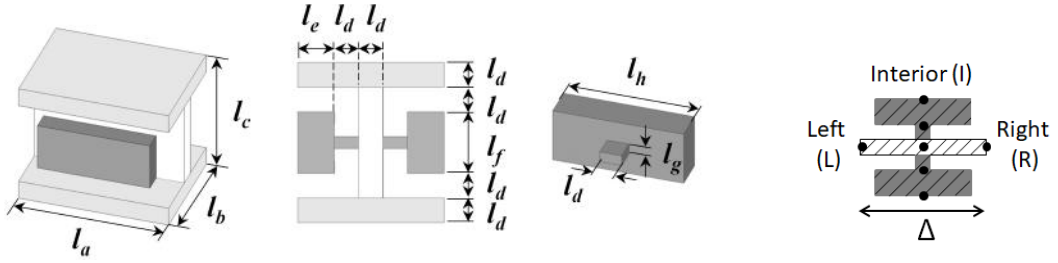

Figure 3: (a) Representation of the metamaterial unit cell with cross-section view and resonator details, and (b) SE meshing with left, right and interior nodes.

Figure 4 shows the dispersion relations of the periodic unit cell with and without resonators. Since $2n\pi \pm \mu$, with n a integer number, are also a solutions of the transfer matrix eigenproblem, only $0 \leq \Re\{\mu\} \leq \pi$, i.e. the Irreducible Brillouin zone, is shown. From the homogeneous beam results in Fig. 4 (a), the two vertical and lateral flexural wave modes are related to propagating (real positive part) and evanescent (imaginary negative part) waves, while the longitudinal and

Table 1: Polyamide nominal mechanical properties of the I-beam and the attached resonators.

Property	I-beam	Resonator mass	Resonator spring
Young' modulus (GPa)	0.86	0.86	0.72
Density (kg/m^3)	700	1000	700
Poisson coefficient	0.39	0.39	0.39
Loss factor	0.03	0.03	0.03

torsional wave modes are propagating only. For the metamaterial beam, Fig. 4 (b), it can be noticed that each wave mode has a significant imaginary component at frequencies corresponding to the stop band around the resonator frequency. This means that the corresponding waves rapidly decay, thus there is vibration attenuation in the band gap. Additionally, the flexural and torsional vibration of the resonator create band gaps in the torsional and in the vertical flexural wave modes, also inducing vibration attenuation zones.

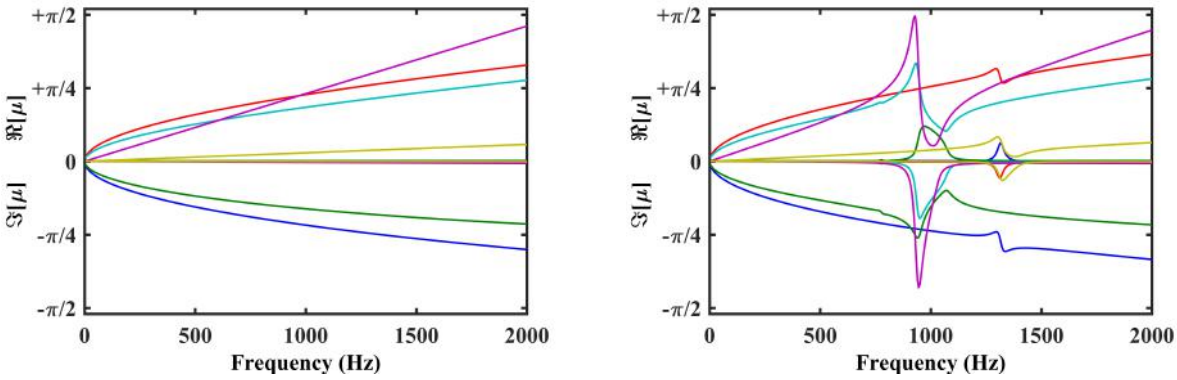

(a) (b)

Figure 4: Complex band structure for the straight beam (a) and the metamaterial beam (b), where the positive and negative values correspond, respectively, to propagating (real) and evanescent (imaginary) components of the wavenumbers related to the vertical bending 1 (cyan), vertical bending 2 (green), lateral bending 1 (red), lateral bending 2 (blue), longitudinal (yellow) and torsional (magenta) wave modes.

4.1 SPATIALLY CORRELATED RESONATORS MISTUNING

In this section, two different cases of Young's modulus spatial variability are presented, namely cases 1 and 2, represented in Fig. 5(a). The forced response is calculated using the full SE method, i.e., each unit cell is given by an SE assembly with constant properties and a full dynamic stiffness matrix is constructed similarly to a standard FE procedure. The harmonic displacements of the finite structure ($\mathbf{q}_{\mathtt{G}}(\omega)$) are computed after the assembly of the global dynamic stiffness matrix ($\mathbf{D}_{\mathtt{G}}(\omega)$) as well as by imposing harmonic external forces ($\mathbf{f}_{\mathtt{G}}(\omega)$) and boundary conditions. The assembly process can be written as $\mathbf{D}_{\mathtt{G}}(\omega) = \boldsymbol{\mathcal{A}}_{\mathtt{s}=1}^{\mathtt{N}}\mathbf{D}_{\mathtt{s}}$, where $\boldsymbol{\mathcal{A}}$ is the finite element-like assembly operator for N unit cells, moreover $\mathbf{D}_{\mathtt{s}}$ is the condensed dynamic stiffness matrix of the unit cell described with SE. Therefore, the spectral displacements are achieved by solving the linear system $\mathbf{q}_{\mathtt{G}}(\omega) = \mathbf{D}_{\mathtt{G}}(\omega)^{-1}\mathbf{f}_{\mathtt{G}}(\omega)$. Additionally, the slowly varying approach, described in Section 2.2is also used to calculate the phase and attenuation change using $N_{gl} = 8$ points for all cases and the forced response is calculated using the approach proposed by Fabro *et al.* (2019). Figure 5(c-d) presents the amplitude of the transfer receptance of the metamaterial beam with non-homogeneous Young's modulus as shown in Fig. 5(a). It can be seen that the slowly varying approach has a very good agreement with the full SE model, except for case (d) in the band gap region.

It can be noticed that the band gap performance is very sensitive to the spatial variation profile and overall spatial level of dispersion. In general, a slight increase in the level of dispersion has the effect of decreasing the level of vibration suppression, while the spatial variability profile has the effect of changing the band gap width. This effect can be explained from the total phase and attenuation changes, shown in Fig. 5(b). For increasing dispersion, the change in attenuation, given by the negative axis of the figure, is smaller. However, the change in spatial variability profile affects the width of the imaginary part. Case 2 has a larger net change of Young's modulus than case 1. This net change has the effect of further decreasing the level of vibration suppression but it also generates a wider bandwidth of vibration attenuation. This variability in the Young's modulus promotes a mistuning around the designed fundamental frequency of the resonators therefore creating an effect similar to a rainbow metamaterial (Zhu *et al.*, 2013). In fact, the spatial profile of the resonators can be optimized to improve the vibration attenuation performance of the metastructure (Meng *et al.*, 2019). The mismatch

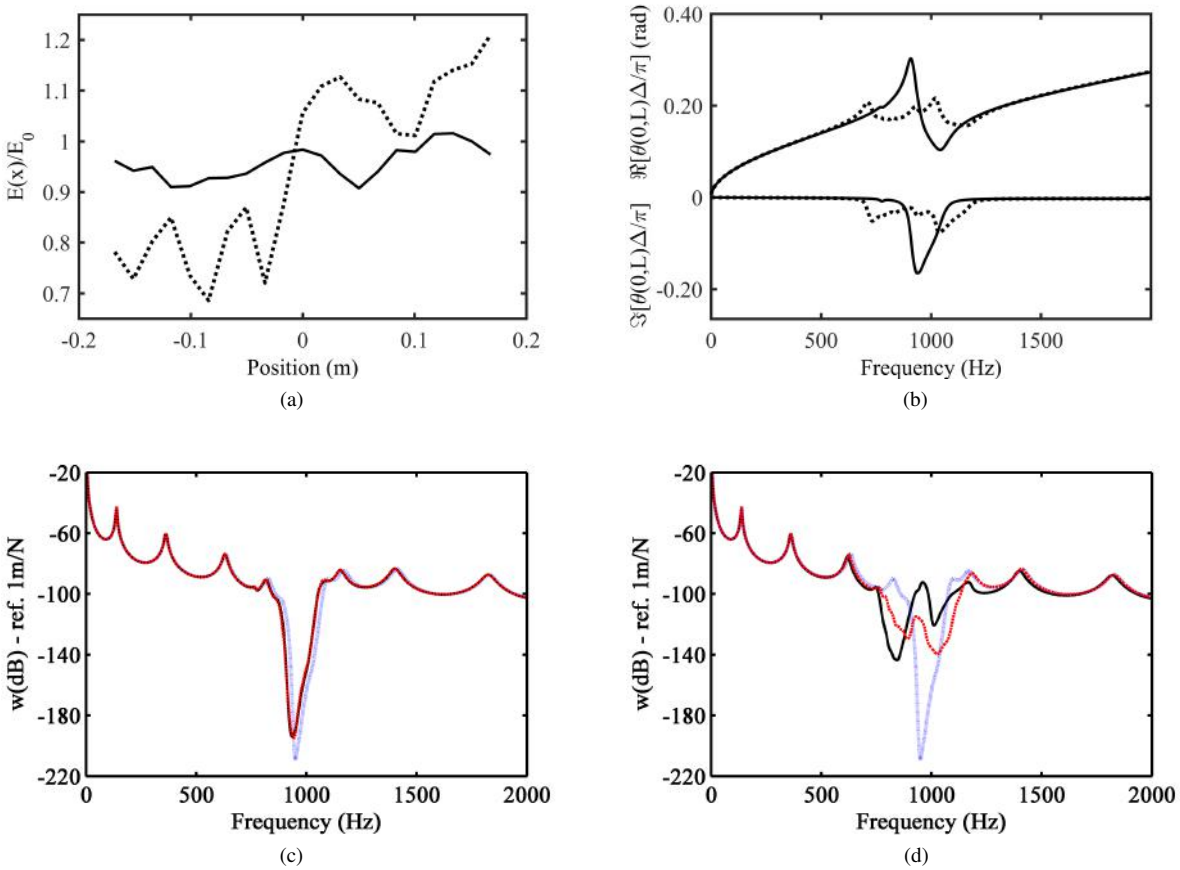

Figure 5: (a) Young's modulus at the resonators as function of the position along the metamaterial beam and (b) phase change (positive) and attenuation (negative) over the metamaterial beam length with variable resonators flexural stiffness for case 1 (full line) and case 2 (dashed line). Amplitude of the transfer receptance of the metamaterial beam with periodic (blue dotted line) and non-periodic Young's modulus with the slowly varying approach (black line) and the full SE method (red line) for (c) case 1 and (d) case 2.

in the amplitude of the transfer receptance from the slowly varying approach and the full SE method, Fig.5(d) suggests that there is at the formation of at least one turning point along the beam in the attenuation frequency range, therefore wave localization (Luongo, 1992). These numerical results confirms and broaden the explanation the experimental results obtained by Beli *et al.* (2019), briefly presented in the previous section.

5. CONCLUDING REMARKS

In summary, the experimental and numerical dynamic behavior of several metamaterial beams constructed in 3D printers were investigated by using deterministic and stochastic approaches. The additive manufacturing process induces material property variability with spatially correlated random distributions. It is shown that depending on the level of disorder, the attenuation bandwidth can be enlarged or annihilated; in addition, the variability can also lead to wave trapping phenomena.

Moreover, it is shown that the spatial profile of the variability plays an important role on the vibration attenuation performance. The phase and attenuation change over the beams length shows the presence of critical sections, known as turning points in the WKB context, which can drastically change the frequency bandwidth and maximum attenuation of the band gap. A critical section is created in the transition between zones of propagating and non-propagating waves at a given frequency and they typically appear in a band around cut-on/cut-off frequencies and at the edges of wave locking and veering.

Although the slowly varying approach is not an accurate representation of the response in the presence of critical sections, due to the consequent wave reflections, it is still possible to investigate the vibration attenuation performance with the phase and attenuation change analysis.

6. ACKNOWLEDGEMENTS

The authors would like to thank the NT3D group from CTI Renato Archer Brazilian Institute (Campinas-SP, Brazil) for manufacturing the metamaterial beam samples through the ProEXP program, and the Nondestructive Testing Laboratory (LabEND) from FEAGRI/UNICAMP for providing the ultrasound equipment used to measure the elastic properties of the cube specimens. The authors also grateful to the Sao Paulo Research Foundation (FAPESP - Sao Paulo, Brazil), through project numbers 2014/19054- 6 and 2015/15718-0, the Federal District Research Foundation (FAPDF - Distrito Federal, Brazil), process number 0193.001507/2017, and the Coordination for the Improvement of Higher Education Personnel (CAPES - Brazil) for the financial support.

7. REFERENCES

Anderson, P.W., 1958. "Absence of Diffusion in Certain Random Lattices". *Physical Review*, Vol. 109, No. 5, pp. 1492–1505. doi:10.1103/PhysRev.109.1492.

Beli, D., Fabro, A.T., Ruzzene, M. and Arruda, J.R.F., 2019. "Wave attenuation and trapping in 3d printed cantilever-in-mass metamaterials with spatially correlated variability". *Scientific Reports*, Vol. 9, No. 1, p. 5617. ISSN 2045-2322. doi:10.1038/s41598-019-41999-0.

Bertoldi, K., Vitelli, V., Christensen, J. and van Hecke, M., 2017. "Flexible mechanical metamaterials". *Nature Reviews Materials*, Vol. 2, No. 17066, p. 11. doi:10.1038/natrevmats.2017.66.

Biggs, N.R.T., 2012. "Wave trapping in a two-dimensional sound-soft or sound-hard acoustic waveguide of slowly-varying width". *Wave Motion*, Vol. 49, pp. 24–33. ISSN 0165-2125. doi:10.1016/j.wavemoti.2011.06.004. 1.

Brillouin, L., 1953. *Wave Propagation in Periodic Structures: Eletric Filters and Crystal Lattices*. Dover Publications. ISBN 0-486-49556-6.

del Barco, O. and Ortuño, M., 2012. "Localization length of nearly periodic layered metamaterials". *Physical Review A*, Vol. 86, p. 023846. doi:10.1103/PhysRevA.86.023846.

Doyle, J., 1997. *Wave Propagation in Structures: Spectral Analysis Using Fast Discrete Fourier Transforms*. Mechanical Engineering Series. Springer New York. ISBN 9780387949406.

Duhamel, D., Mace, B. and Brennan, M., 2006. "Finite element analysis of the vibrations of waveguides and periodic structures". *Journal of Sound and Vibration*, Vol. 294, No. 1, pp. 205 – 220. ISSN 0022-460X. doi:10.1016/j.jsv.2005.11.014.

Fabro, A.T., Beli, D., Arruda, J.R.F., Ferguson, N.S. and Mace, B., 2016a. "Uncertainty analysis of band gaps for beams with periodically distributed resonators produced by additive manufacturing". In *ISMA 2016 Conference on Noise and Vibration Engineering*. Leuve, Belgium, p. 12.

Fabro, A.T., Ferguson, N.S. and Mace, B.R., 2016b. "Flexural Wave Propagation in Slowly Varying Random Waveguides Using a Finite Element Approach". *Journal of Physics: Conference Series*, Vol. 744, No. 1, p. 012198. ISSN 1742-6596. doi:10.1088/1742-6596/744/1/012198.

Fabro, A.T., Ferguson, N.S. and Mace, B.R., 2019. "Wave propagation in slowly varying waveguides using a finite element approach". *Journal of Sound and Vibration*, Vol. 442, pp. 308–329. ISSN 0022-460X. doi:10.1016/j.jsv.2018.11.004.

Fabro, A.T., Ferguson, N.S., Jain, T., Halkyard, R. and Mace, B.R., 2015. "Wave propagation in one-dimensional waveguides with slowly varying random spatially correlated variability". *Journal of Sound and Vibration*, Vol. 343, pp. 20–48. ISSN 0022-460X. doi:10.1016/j.jsv.2015.01.013.

Goodridge, R., Tuck, C. and Hague, R., 2012. "Laser sintering of polyamides and other polymers". *Progress in Materials Science*, Vol. 57, No. 2, pp. 229 – 267. ISSN 0079-6425. doi:10.1016/j.pmatsci.2011.04.001.

Hague, R., Campbell, I. and Dickens, P., 2003. "Implications on design of rapid manufacturing". *Proceedings of the Institution of Mechanical Engineers, Part C: Journal of Mechanical Engineering Science*, Vol. 217, No. 1, pp. 25–30. doi:10.1243/095440603762554587.

Hu, H., Ji, D., Zeng, X., Liu, K. and Gan, Q., 2013. "Rainbow trapping in hyperbolic metamaterial waveguide". *Scientific Reports*, Vol. 3, p. 1249. doi:10.1038/srep01249.

Hussein, M.I., Leamy, M.J. and Ruzzene, M., 2014. "Dynamics of phononic materials and structures: Historical origins, recent progress, and future outlook". *Applied Mechanics Reviews*, Vol. 66, No. 4, pp. 040802–040802–38. doi:10.1115/1.4026911.

Lee, S.K., Mace, B. and Brennan, M., 2007. "Wave propagation, reflection and transmission in non-uniform one-dimensional waveguides". *Journal of Sound and Vibration*, Vol. 304, No. 1, pp. 31 – 49. ISSN 0022-460X. doi:10.1016/j.jsv.2007.01.039.

Lee, U., 2009. *Spectral Element Method in Structural Dynamics*. Wiley. ISBN 9780470823750.

Liu, Z., Zhang, X., Mao, Y., Zhu, Y.Y., Yang, Z., Chan, C.T. and Sheng, P., 2000. "Locally resonant sonic materials". *Science*, Vol. 289, No. 5485, pp. 1734–1736. ISSN 0036-8075. doi:10.1126/science.289.5485.1734.

Lu, M.H., Feng, L. and Chen, Y.F., 2009. "Phononic crystals and acoustic metamaterials". *Materials Today*, Vol. 12, No. 12, pp. 34 – 42. ISSN 1369-7021. doi:10.1016/S1369-7021(09)70315-3.

Luongo, A., 1992. "Mode localization by structural imperfections in one-dimensional continuous systems". *Journal of Sound and Vibration*, Vol. 155, No. 2, pp. 249–271. ISSN 0022-460X. doi:10.1016/0022-460X(92)90510-5.

Ma, G. and Sheng, P., 2016. "Acoustic metamaterials: From local resonances to broad horizons". *Science Advances*, Vol. 2, No. 2, p. e1501595. doi:10.1126/sciadv.1501595.

Mace, B.R., Duhamel, D., Brennan, M.J. and Hinke, L., 2005. "Finite element prediction of wave motion in structural waveguides". *The Journal of the Acoustical Society of America*, Vol. 117, No. 5, pp. 2835–2843. doi: 10.1121/1.1887126.

Maldovan, M., 2013. "Sound and heat revolutions in phononics". *Nature*, Vol. 503, p. 209. doi:10.1038/nature12608.

Mencik, J.M. and Ichchou, M.N., 2005. "Multi-mode propagation and diffusion in structures through finite elements". *European Journal of Mechanics - A/Solids*, Vol. 24, No. 5, pp. 877–898. ISSN 0997-7538. doi: 10.1016/j.euromechsol.2005.05.004.

Mencik, J.M. and Ichchou, M.N., 2008. "A substructuring technique for finite element wave propagation in multi-layered systems". *Computer Methods in Applied Mechanics and Engineering*, Vol. 197, No. 6, pp. 505–523. ISSN 0045-7825. doi:10.1016/j.cma.2007.08.002.

Meng, H., Chronopoulos, D. and Fabro, A.T., 2019. "Optimal design of a rainbow metamaterial". In *Proceedings of the 26th International Congress on Sound and Vibration - ICSV26*. Montreal, Canada.

Morsbol, J.O., Sorokin, S.V. and Peake, N., 2016. "A WKB approximation of elastic waves travelling on a shell of revolution". *Journal of Sound and Vibration*, Vol. 375, No. Supplement C, pp. 162–186. ISSN 0022-460X. doi: 10.1016/j.jsv.2016.04.001.

Nielsen, R.B. and Peake, N., 2016. "Tunnelling effects for acoustic waves in slowly varying axisymmetric flow ducts". *Journal of Sound and Vibration*, Vol. 380, pp. 180–191. ISSN 0022-460X. doi:10.1016/j.jsv.2016.06.003.

Pierce, A.D., 1970. "Physical interpretation of the wkb or eikonal approximation for waves and vibrations in inhomogeneous beams and plates". *The Journal of the Acoustical Society of America*, Vol. 48, No. 1B, pp. 275–284. doi:10.1121/1.1912125.

Renno, J.M. and Mace, B.R., 2010. "On the forced response of waveguides using the wave and finite element method". *Journal of Sound and Vibration*, Vol. 329, pp. 5474–5488. ISSN 0022-460X. doi:10.1016/j.jsv.2010.07.009. 26.

Sugino, C., Xia, Y., Leadenham, S., Ruzzene, M. and Erturk, A., 2017. "A general theory for bandgap estimation in locally resonant metastructures". *Journal of Sound and Vibration*, Vol. 406, No. Supplement C, pp. 104–123. ISSN 0022-460X. doi:10.1016/j.jsv.2017.06.004.

Trainiti, G., Rimoli, J.J. and Ruzzene, M., 2018. "Optical evaluation of the wave filtering properties of graded undulated lattices". *Journal of Applied Physics*, Vol. 123, No. 9, p. 091706. doi:10.1063/1.5011369.

Vanmarcke, E., 2010. *Random Field: Analysis and Synthesis*. Word Scientific, Cambridge, MA, 2nd edition. ISBN 13 978-981-256-297-5.

Zhu, J., Christensen, J., Jung, J., Martin-Moreno, L., Yin, X., Fok, L., Zhang, X. and Garcia-Vidal, F.J., 2010. "A holey-structured metamaterial for acoustic deep-subwavelength imaging". *Nature Physics*, Vol. 7, pp. 52–55. doi: 10.1038/nphys1804.

Zhu, J., Chen, Y., Zhu, X., Garcia-Vidal, F.J., Yin, X., Zhang, W. and Zhang, X., 2013. "Acoustic rainbow trapping". *Scientific Reports*, Vol. 3, p. 1728. ISSN 2045-2322. doi:10.1038/srep01728.

8. RESPONSIBILITY NOTICE

The authos are the only responsible for the printed material included in this paper.